Special Collection

Photoswitchable 2-Phenyldiazenyl-Purines and their Influence on DNA Hybridization

Nikolai Grebenovsky,[a] Volker Hermanns,[a] and Alexander Heckel*[a]

Recently, photochromic derivatives of nucleobases have drawn attention for regulating oligonucleotide hybridization with light for photopharmacological applications. The nucleobase moiety provides attractive interaction for hybridization, whereas the photochromic moiety can alter the interaction upon irradiation due to conformational changes. Herein we report the synthesis of 2-phenyldiazenyl-substituted 2′-deoxyadenosine (**dA$_{Azo}$**) and 2′-deoxyguanosine (**dG$_{Azo}$**) and investigate their influence in a DNA context by UV/Vis absorption, fluorescence and CD spectroscopies. For comparison, the literature-known azobenzene *C*-nucleoside **DNAzo** was used as a reference system. It could be shown that photochromic purines improve overall hybridization affinity compared to azobenzene *C*-nucleosides. In particular, 2′-deoxyadenosine analogue dA$_{Azo}$ increases melting temperatures by 7.5 °C in the favored *trans* state with 86% of the switching efficiency of the reference system.

The interaction of oligonucleotides are very precise and well defined. The knowledge of their interaction patterns gave us insight into fundamental biological processes such as transcription and translation of genetic information into gene products and regulation of this process. External regulation of oligonucleotide hybridization through a stimulus enables interesting applications both on a mechanistic and even on a therapeutic level. Utilizing light is an elegant way to gain control over hybridization processes. Light does not pollute the system of interest, can be applied with high spatio-temporal resolution and is not harmful in a biological context, if power and wavelength are controlled.[1–4] Several approaches paved the way to design modern tools for photopharmacological applications, such as spatiotemporal control of angiogenesis,[5,6] CRISP/Cas9[7] and many others.[8–10]

One strategy is the utilization of photochromic derivatives of natural nucleobases (e.g. derived from photoswitches) for applying light control to base pairing of oligonucleotides. The nucleobase moiety provides attractive interaction for hybridization, whereas the photochromic moiety can alter the interaction upon irradiation due to conformational changes. Besides different studies with spiropyrans[11,12,13] and diarylethenes[14] used as photoswitches, Stilbene modifications of purines and pyrimidines are known. The *cis-trans*-photoisomerization of stilbene-modified nucleobases have been used in photochemical studies,[15–17] to regulate G-quadruplex formation[18] and even as a photoresponsive 5′-cap structure to control protein expression.[19] Unfortunately, *trans*-to-*cis*-photoisomerization requires wavelengths of around 310 nm, which can cause photodamage in biological tissue.

Azobenzenes have a great potential for oligonucleotide applications. They are easy to synthesize,[20] their photophysical properties can be custom-tailored to the application's requirements[5] and therefore have already been used in numerous studies involving oligonucleotides.[21] Attaching the azobenzene onto nucleobases via amid- or alkyl linkers to create simple photochromic nucleobases leads to only little photocontrol, as the chromophore points into the major groove.[22,23] The way of incorporating the azobenzene into the nucleobase is of utmost importance, as it has to provide a rigid base for the isomerization movement. In addition, the azobenzene needs to be positioned in the base pair stack without the possibility to evade into the minor or major groove during isomerization. Replacing nucleobases with azobenzenes to create azobenzene *C*-nucleosides does exactly that and has been shown to regulate hybridization in DNA, RNA and DNA-nanostructures.[24–27] Apparently, introducing azobenzene as a nucleobase substitute implies a steric disturbance in the duplex even in the favored *trans*-state, which results in decreased binding affinity.

Wang *et al.* added a thymidine-like residue to the distal aromatic ring of an azobenzene *C*-nucleoside to allow hydrogen bonding in the *trans*-state, whereas the *cis*-state decreases base pairing affinity by steric hindrance. This system could be shown to regulate oligonucleotide hybridization, although the large photochromic nucleobase causes a lot of steric hindrance in the base pairing region.[28] Recently, 2-phenyldiazenyl-7-methyl-guanosine has been developed and used as a photoresponsive 5′-cap *in vivo* to control protein expression in a time-resolved manner.[29] Upon *trans*-to-*cis* isomerization, expression of the squint protein in zebrafish embryos could be increased by a factor of 7.1, demonstrating that the position of the distal aromatic ring on the 2-phenyldiazenyl-7-methyl-guanosine has great impact on enzyme recognition. Although demonstrated for enzymatic interactions, the effect on oligonucleotide hybridization stays unclear to this date. It can be

[a] Dr. N. Grebenovsky, V. Hermanns, Prof. Dr. A. Heckel
Institute for Organic Chemistry and Chemical Biology
Goethe-University Frankfurt
Max-von-Laue-Straße 7
D-60438 Frankfurt am Main (Germany)
E-mail: heckel@uni-frankfurt.de

Supporting information for this article is available on the WWW under https://doi.org/10.1002/cptc.202000162

An invited contribution to a Special Collection on Photopharmacology

assumed that the position of the distal aromatic ring in a confined space like the base pairing region of an oligonucleotide duplex will cause steric hindrance depending on its conformation. In the *trans*-state, the distal aromatic ring will be positioned in the minor-groove. During *cis*-to-*trans* isomerization it is unclear if the distal aromatic ring can shift into the base pairing region, thereby weakening hydrogen bonding of adjacent base pairs, or stays in the minor groove with a non-natural C–N=N–C dihedral angle. This depends on the partially rotatable C2–N-Bond and the original positioning of the distal ring in its *trans*-state, as two different conformations exist with the distal ring either being in close proximity to the base-pairing region (endo) or in greater distance (exo, Figure 1).

To investigate this, 2-phenyldiazenyl substituted analogues of 2′-deoxyadenosine- and 2′-deoxyguanosine-phosphoramidites have been synthesized for introduction into oligonucleotides by solid phase synthesis. The literature-known azobenzene *C*-nucleoside **DNAzo** was used as a reference to compare the influence on oligonucleotide hybridization. In order to prepare 2-aryldiazenylpurine compounds by a Mills-reaction, the reaction of an electron deficient amine and a nitroso-compound under acidic conditions could be used. As the C-2 position in purines is rather electron rich, a route via 2-nitrosopurines was chosen. In analogy to the approach of Wanner *et al.*[30] 2-nitrosopurines were prepared from acetyl-protected 2′-deoxyadenosine **2** by chlorinating C-6 position (**3**) and nitration of the C-2 position (**4**, Figure 2). The nitration was followed by hydrogenation to form the hydroxylamine **5** as an intermediate, which was subsequently oxidized with sodium periodate to form protected 2-nitroso-6-chloropurine **6** as coupling reagent. Upon reaction with aniline, 2-phenyldiazenyl-6-chloropurine **7** could be formed under Mills-conditions. At this point, either adenosine or guanosine derivatives could be synthesized from the same compound, which is an advantage of this synthetic pathway. To incorporate unprotected 2-phenyldiazenylpurine nucleosides **8** or **11** into oligonucleotides by solid-phase synthesis, phosphoramidites where prepared by tritylation (compounds **9** and **12**) and successive phosphitylation (compounds **10** and **13**). The **DNAzo** phosphoramidite

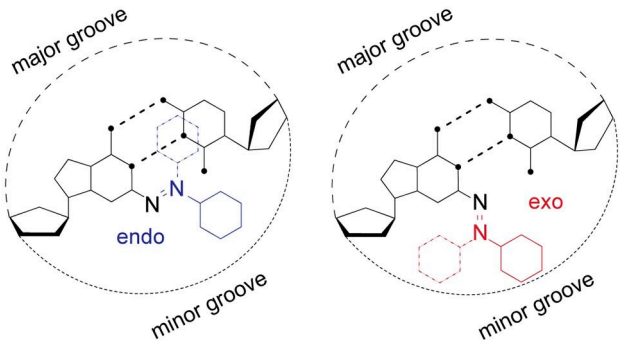

Figure 1. Schematic drawing of a general 2-phenyldiazenylpurine incorporated into an oligonucleotide hybridizing with a complementary nucleobase in top view. The two different *trans* states would most likely result in different conformational changes of the distal aromatic ring upon photoisomerization (dashed aryl residue).

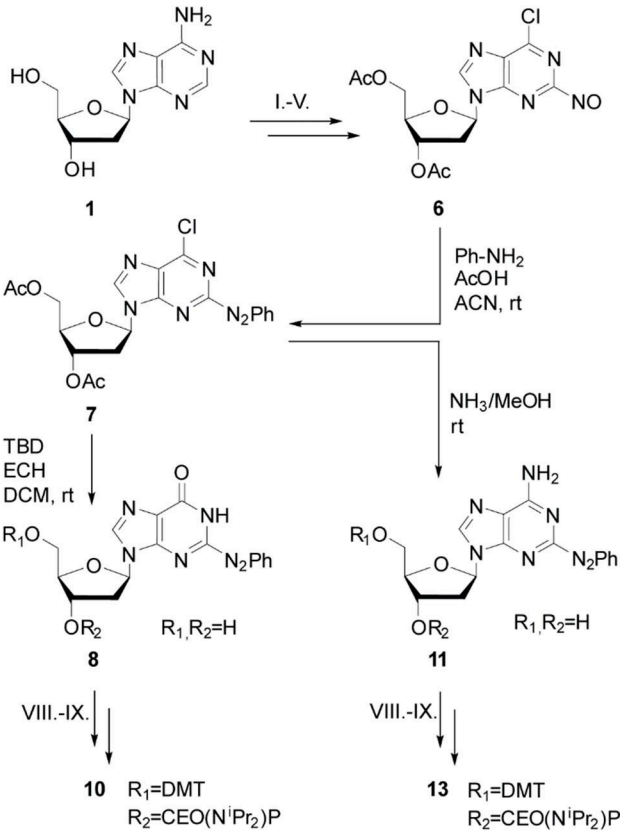

Figure 2. Synthetic route to obtain 2-phenyldiazenylpurine nucleosides and their conversion to phosphoramidites for solid phase synthesis (Conditions I: Ac_2O, DMAP, TEA, ACN 0 °C; II: AcCl, TBN, DCM, rt; III: TBAN, TFAA, DCM, 0 °C; IV: Pd/C, H_2, EA, rt; V: $NaIO_4$, EA/H_2O, rt; VIII: DMTCl, py 0 °C→rt; IX: CEO (N^iPr_2)PCl, DIPEA, DCM, rt.).

used as reference in this study was synthesized as previously published.[26]

With compounds **8** (dG_{Azo}) and **11** (dA_{Azo}) in our hands, first we started the photochemical characterization of the free nucleosides. We determined the spectra of the pure photoisomers of both compounds by separating them via RP-HPLC (see Supporting Figures S3 and S4). In both cases, the *trans*-isomer shows a higher extinction coefficient than the *cis*-isomer above the isosbestic point at 278 nm. Photostationary states were recorded at different wavelengths between 310 and 505 nm (see Supporting Information, section 3). Photofatigue was tested in PBS-buffer over 100 switching cycles and showed no significant degradation. At 37 °C dG_{Azo} and dA_{Azo} showed both only very slow thermal relaxation rates of the *cis*-state to the thermodynamically favored *trans*-state of $k = 0.034 \pm 0.001\ s^{-1}$ for dG_{Azo} and $k = 0.14 \pm 0.02\ s^{-1}$ for dA_{Azo} (see Supporting Information, section 3.5).

Finally, the quantum yields of the individual photoreactions were determined at 455 nm for the *cis-to-trans* reaction (58.9 ± 0.2 % for dG_{Azo} and 43.5 ± 0.5 % for dA_{Azo}) and at 365 nm for the *trans-to-cis* reaction (18.7 ± 0.1 % for dG_{Azo} and 16.9 ± 0.2 % for dA_{Azo}) (see Supporting Information, section 3.6).

To test the impact of the 2-phenyldiazenylpurines and their photoisomers, a DNA model sequence with a 60 % GC-content

was chosen. The sequence was set to a length of 10 nucleotides in order to evaluate the impact of a single modification incorporated into the oligonucleotide (Figure 3a,b). Fluorescein and Dabcyl residues as fluorophore-quencher-pair where installed at one end of the duplex to obtain melting temperature data from both fluorescence readout as well as UV/vis measurements. In addition, changes in the helical structure of the duplex was investigated by means of CD-spectroscopy.

From the UV/vis-absorption data, it could be seen that **DNAzo** as a reference system decreases the melting temperature by 16.4 °C compared to the unaltered wild type (Figure 3c). Exchanging the **DNAzo** residue for the guanosine-analogue **dG_{Azo}**, the melting temperature increased by 3.4 °C, incorporating the adenosine-analogue **dA_{Azo}** into the counter strand led to an overall increase of 7.5 °C. This appears to fit expectations, as 2-phenyldiazenylpurines should increase affinity due to their own base pairing capabilities. The melting temperatures for **dG_{Azo}** are somewhat lower than when dA_{Azo} is used. This is also not unexpected, since introducing the phenyldiazenyl residue replaces the 2-amino residue in 2′-deoxyguanosine, which reduces hydrogen bonding capabilities. 2′-Deoxyadenosine carries no functionality on the C-2 position, so that addition of the phenyldiazenyl residue does not alter hydrogen bonding capabilities. The influence of the photoswitching for the literature-known **DNAzo** residue in this sequence context is a difference of 1.5 °C between the photostationary states at 455 nm and 365 nm ($\triangle T_M$). The melting temperature difference is only 0.5 °C for **dG_{Azo}** and 1.3 °C for dA_{Azo}. It appears, that the reorientation of the distal aromatic ring does not change hydrogen bonding for **dG_{Azo}** significantly, supporting the idea closer that the *trans*-to-*cis*-isomerization happens most likely in the minor groove. The photoisomerization of **dA_{Azo}** is less effective than for **DNAzo**, but influences hybridization more than **dG_{Azo}**. As final test, **dG_{Azo}**- and **dA_{Azo}**-including strands were hybridized to test their combined influence in a so called dimer-motif. The melting temperature was lower than for **DNAzo** (by 2.6 °C) and photoswitching resulted in as much difference as with **dG_{Azo}** alone. CD-spectroscopy revealed that the strongest difference in helicity between the photostationary states could be seen for **DNAzo** (see Supporting Information, section 5). 2-Phenyldiazenylpurines did not alter B-DNA helicity compared to the wild type significantly, which might explain why they do not influence hybridization behavior in the same extend as **DNAzo**. In addition to measuring melting curves with UV/vis-absorption, temperature-dependent fluorescence was measured in a real-time PCR device for all duplexes in a concentration range of 0.1 μM to 5 μM. The results were in overall accordance with values from UV/vis-absorbance. Fluorescence-based melting temperatures are listed in the Supporting Information, section 6.

In summary, we have synthesized 2-phenyldiazenyl substituted analogues of 2′-deoxyguanosine and 2′-deoxyadenosine, characterized them photochemically and incorporated them into DNA. The melting curves showed that the new building blocks increase hybridization affinity compared to the literature known **DNAzo** with the adenosine analogue even more than the guanosine analogue. $\triangle T_M$ values of dA_{Azo} was slightly smaller, for dG_{Azo} much smaller than for the reference system. This gives insight into this emerging class of photochromic nucleobases, which could be used for future applications in photochromic DNA-materials, gene expression control or photopharmacology.

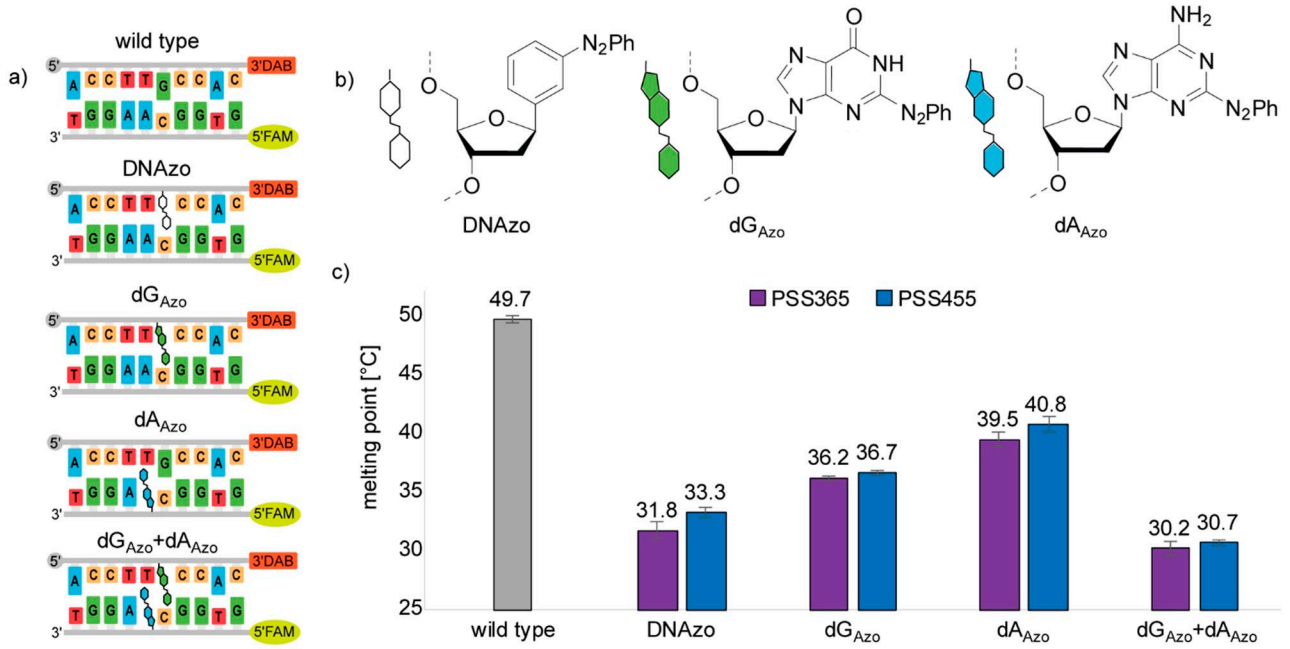

Figure 3. Schematic display of DNA strands used in this study (a), incorporated photochromic modifications (b) and melting temperatures measured by UV/Vis absorption spectroscopy (c).

Experimental Section

Organic syntheses including spectroscopic data are described in detail in the Supporting Information, section 1. Oligonucleotide synthesis, including mass spectroscopic data, are included in the Supporting Information section 2. Section 3 shows photophysical characterization data of the 2-phenyldiazenyl substituted nucleosides **8** and **11**. This includes spectra of the photostationary states and pure photoisomers, photostationary distributions, photofatigue studies, thermal relaxation of the cis-isomers and quantum yields of the photochemical processes. The quantum yield determination was carried out according to Reinfelds *et al.*[31] For melting temperature measurements 1 mL samples were prepared with a 1 μM concentration of strand and counter strand in 1x PBS-buffer for the 5 different duplexes. The absorbance changes at 260 nm were measured in a UV/vis-spectrometer from JASCO. Samples were irradiated as single strands at 80 °C with either 365 nm or 455 nm until the photostationary state (PSS) was reached to prevent mismatches. A temperature gradient of 1 °C per minute was used. To avoid effects of hysteresis, melting temperatures were calculated by sigmoidal fit from cooling and heating measurements. At least five independent heating and cooling measurements were performed for precise results. Temperature-dependent fluorescence measurements were recorded in a PikoReal real-time PCR system (*Thermo Scientific*). Triplicates were irradiated at 80 °C, then spectra were measured from 80 °C to 5 °C within one hour. Values given were averaged over these three individual samples.

Acknowledgements

This work was supported by the Deutsche Forschungsgemeinschaft through SFB 902 ("Molecular Principles of RNA-Based Regulation") and GRK 1986 ("Complex Light-Control") Open access funding enabled and organized by Projekt DEAL.

Conflict of Interest

The authors declare no conflict of interest.

Keywords: azo compounds · DNA · oligonucleotides · photochromism · photopharmacology

[1] N. Ankenbruck, T. Courtney, Y. Naro, A. Deiters, *Angew. Chem. Int. Ed.* **2018**, *57*, 2768–2798; *Angew. Chem.* **2018**, *130*, 2816–2848.
[2] C. Brieke, F. Rohrbach, A. Gottschalk, G. Mayer, A. Heckel, *Angew. Chem. Int. Ed.* **2012**, *51*, 8446–8476; *Angew. Chem.* **2012**, *124*, 8572–8604.
[3] W. Szymański, J. M. Beierle, H. A. V. Kistemaker, W. A. Velema, B. L. Feringa, *Chem. Rev.* **2013**, *113*, 6114–6178.
[4] P. Klán, T. Šolomek, C. G. Bochet, A. Blanc, R. Givens, M. Rubina, V. Popik, A. Kostikov, J. Wirz, *Chem. Rev.* **2013**, *113*, 119–191.
[5] M. Dong, A. Babalhavaeji, S. Samanta, A. A. Beharry, G. A. Woolley, *Acc. Chem. Res.* **2015**, *48*, 2662–2670.
[6] T. Lucas, F. Schäfer, P. Müller, S. A. Eming, A. Heckel, S. Dimmeler, *Nat. Commun.* **2017**, *8*, 15162.
[7] W. Zhou, W. Brown, A. Bardhan, M. Delaney, A. S. Ilk, R. R. Rauen, S. I. Kahn, M. Tsang, A. Deiters, *Angew. Chem. Int. Ed.* **2020**, *59*, 8998–9003.
[8] K. Hüll, J. Morstein, D. Trauner, *Chem. Rev.* **2018**, *118*, 10710–10747.
[9] E. Bamberg, W. Gärtner, D. Trauner, *Chem. Rev.* **2018**, *118*, 10627–10628.
[10] A. Deiters, *ChemBioChem* **2018**, *19*, 1198–1200.
[11] C. Özçoban, T. Halbritter, S. Steinwand, L.-M. Herzig, J. Kohl-Landgraf, N. Askari, F. Groher, B. Fürtig, C. Richter, H. Schwalbe, B. Suess, J. Wachtveitl, A. Heckel, *Org. Lett.* **2015**, *17*, 1517–1520.
[12] C. Beyer, H.-A. Wagenknecht, *Synlett* **2010**, *2010*, 1371–1376.
[13] S. Barrois, C. Beyer, H.-A. Wagenknecht, *Synlett* **2012**, *23*, 711–716.
[14] S. Barrois, H.-A. Wagenknecht, *Beilstein J. Org. Chem.* **2012**, *8*, 905–914.
[15] S. Ogasawara, I. Saito, M. Maeda, *Tetrahedron Lett.* **2008**, *49*, 2479–2482.
[16] S. Ogasawara, M. Maeda, *Angew. Chem. Int. Ed.* **2008**, *47*, 8839–8842; *Angew. Chem.* **2008**, *120*, 8971–8974.
[17] S. Ogasawara, M. Maeda, *Nucleic Acids Symp. Ser.* **2008**, *52*, 369–370.
[18] S. Ogasawara, M. Maeda, *Angew. Chem. Int. Ed.* **2009**, *48*, 6671–6674; *Angew. Chem.* **2009**, *121*, 6799–6802.
[19] S. Ogasawara, M. Maeda, *Bioorg. Med. Chem. Lett.* **2011**, *21*, 5457–5459.
[20] E. Merino, *Chem. Soc. Rev.* **2011**, *40*, 3835.
[21] A. S. Lubbe, W. Szymanski, B. L. Feringa, *Chem. Soc. Rev.* **2017**, *46*, 1052–1079.
[22] M. Liu, H. Jinmei, H. Abe, Y. Ito, *Bioorg. Med. Chem. Lett.* **2010**, *20*, 2964–2967.
[23] S. Mori, K. Morihiro, S. Obika, *Molecules* **2014**, *19*, 5109–5118.
[24] T. Goldau, K. Murayama, C. Brieke, S. Steinwand, P. Mondal, M. Biswas, I. Burghardt, J. Wachtveitl, H. Asanuma, A. Heckel, *Chem. Eur. J.* **2015**, *21*, 2845–2854.
[25] T. Goldau, K. Murayama, C. Brieke, H. Asanuma, A. Heckel, *Chem. Eur. J.* **2015**, *21*, 17870–17876.
[26] N. Grebenovsky, T. Goldau, M. Bolte, A. Heckel, *Chem. Eur. J.* **2018**, *24*, 3425–3428.
[27] N. Grebenovsky, L. Luma, P. Müller, A. Heckel, *Chem. Eur. J.* **2019**, *25*, 12298–12302.
[28] R. Wang, C. Jin, X. Zhu, L. Zhou, W. Xuan, Y. Liu, Q. Liu, W. Tan, *J. Am. Chem. Soc.* **2017**, *139*, 9104–9107.
[29] S. Ogasawara, *ACS Chem. Biol.* **2017**, *12*, 351–356.
[30] M. J. Wanner, G.-J. Koomen, *J. Chem. Soc. Perkin 1* **2001**, 1908–1915.
[31] M. Reinfelds, V. Hermanns, T. Halbritter, J. Wachtveitl, M. Braun, T. Slanina, A. Heckel, *ChemPhotoChem* **2019**, *3*, 441–449.

Manuscript received: June 30, 2020
Revised manuscript received: July 20, 2020
Accepted manuscript online: July 22, 2020
Version of record online: August 7, 2020